Atomic scale modeling of austenite-martensite transformation

H. Zapolsky , M. Certain and M. Lavrsky,

GPM, UMR 6634, University of Rouen, France

A.G. Khachaturyan

Rutgers University, NJ, USA

PFM 2014
State College

Martensite transformation (MT) Introduction

A martensitic transformation:

- a first order phase transition that proceeds under conditions where the initial phase maintains metastability.

- The tendency toward stress relaxation leads to the formation of new phase plates with regular orientations and internal substructure (polysynthetic twins or slip packets).

- The plates form regular groups in such a way that the free energy should be at a minimum.

- The austenite/martensite interfaces are invariant under the transformation ->habit plane

↓

Multidomain structure -> two twin-related orientation variants

Self-accommodation by variants

A typical feature of martensitic transformations is that each colony of martensite laths/plates consists of a stack in which different variants alternate. This allows large shears to be accommodated with minimal macroscopic shear.

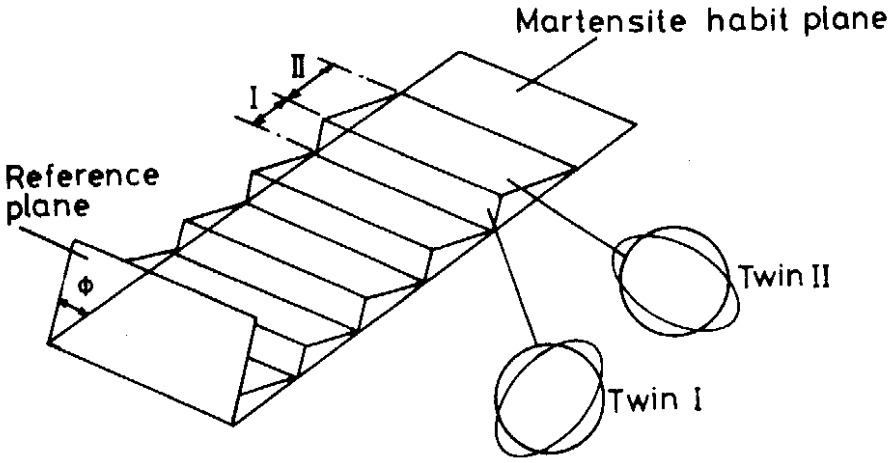

Fig. 6.10 Twins in martensite may be self-accommodating and reduce energy by having alternate regions of the austenite undergo the Bain strain along different axes.

Martensite transformation
Introduction

Nucleation mechanisme of martensite

G.B. Olson and A.L. Roitburd, Martensite (1992).
Y. Wang, A.G. Khachaturyan, Acta.Mat. (1997)
W. Zang, Y.M. Jin, A.G. Khachaturyan, Acta Mat. (2007)

- **The strain energy contribution to the nucleation barrier of a single variant martensitic particle is too high to be overcome by thermal fluctuations ->pre-existening martensitic embryos around a dislocation defect is a complex nanoscale assemblages of martensitic microdomains rather than a homogeneous single-domain particle.**

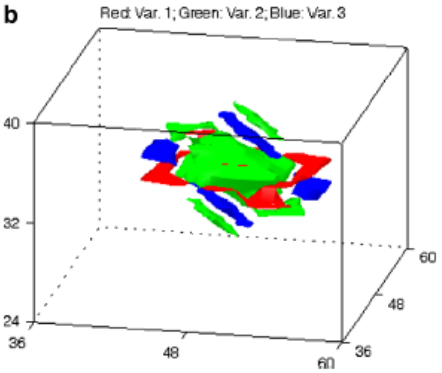

Fig. 3. Metastable martensitic embryos induced by a single dislocation loop ($M=1$) at the time $\tau=2000$: (a) $\Delta\tilde{f}_L^v=0.056$ ($\Delta T\approx 200$ K); (b) $\Delta\tilde{f}_L^v=0.058$ ($\Delta T\approx 207$ K). The same visualization method is used for all plots: parent phase is transparent, $\Delta\tilde{f}_L^v=\eta|_1|\geq 0.7$ in red, $|\eta_2|\geq 0.7$ in green, and $|\eta_3|\geq 0.7$ in blue.

W. Zang, Y.M. Jin,
A.G. Khachaturyan,. (2007)

Objectives

Understand the first stages of MT at atomic scale:

- The microstructural sequence of the development of a martensitic nucleus from the parent phase

Approach:

3D atomic density function modeling

Atomic density function model

Static concentration waves method (A. G. Khachaturyan, 1971)

Occupation probability:

$$p = \bar{c}$$

$$P(r) = \bar{c} + \Delta c(r)$$

$$P(r) = \bar{c} + \frac{1}{2}\sum_j [Q(\vec{k}_j)e^{i\vec{k}_j\cdot\vec{r}} + Q^*(\vec{k}_j)e^{-i\vec{k}_j\cdot\vec{r}}]$$

Amplitudes of static concentration waves ->

$$Q(k_j) = \eta(k_j)\gamma(k_j)$$

Internal energy->

$$U = \frac{N}{2}V(0)c^2 + \frac{N}{2}\sum_j V(k_j)\eta_j^2$$

$$V(k) = \sum_r V(r)e^{-ikr}$$

$$F_{chem} = \frac{1}{2}\sum_{r,r'} V(r-r')p(r)p(r') + k_B T\sum_{\vec{r}}\{p(r)Ln(p(r)) + [1-p(r)]Ln[1-(p(r)]\}$$

Atomic density function model

$$F = F_{chem} + E_{elast}$$

$$E_{elast} = \frac{1}{2}\sum_{pq}\int \frac{d^3k}{(2\pi)^3} B_{pq}(\mathbf{n})\theta_p(\mathbf{k})\theta_q^*(\mathbf{k})$$

Microscopic diffusion equation

$$\frac{dP(r,t)}{dt} = \frac{1}{k_B T}\sum_{\alpha,\beta}\sum_{r'} L_{\alpha\beta}(r-r')c_\alpha c_\beta \frac{\partial F}{\partial P(r',t)}$$

Conserved dynamic with the condition: $\sum_r L(r-r') = 0$

Phases presentation in ADF model on constrained lattice

2D Simulation :

fcc lattice =>square lattice

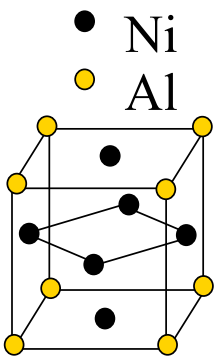

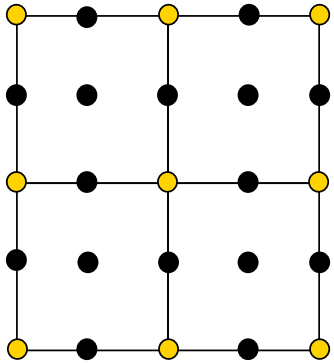

$L1_2$ 2D Projection of $L1_2$

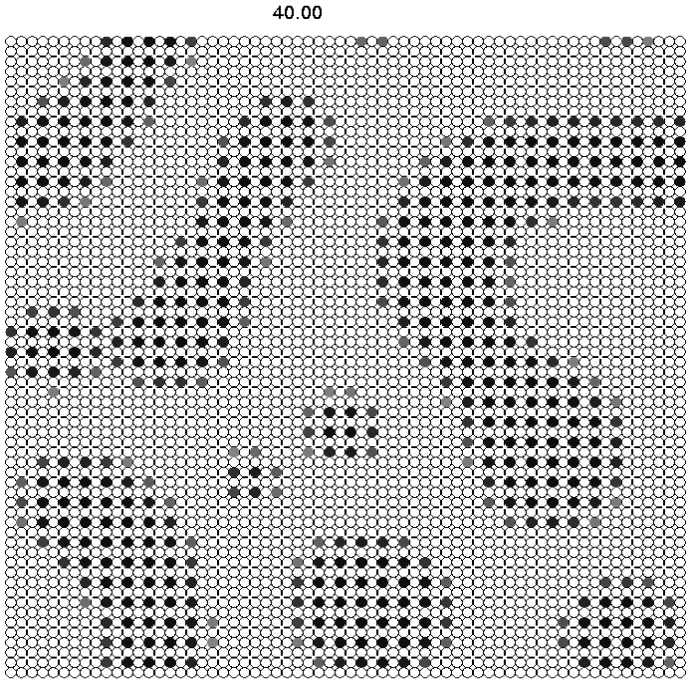

Site probability presentation

Order parameter presentation

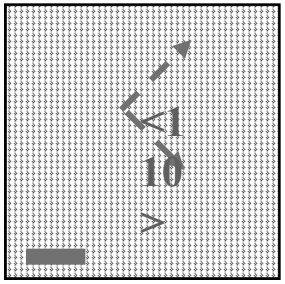

50 nm

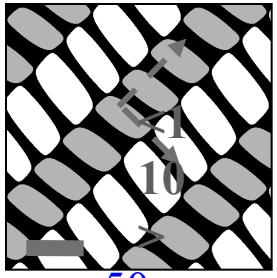

50 nm

d =$\varepsilon_{11}/\varepsilon_{33}$= -0.35

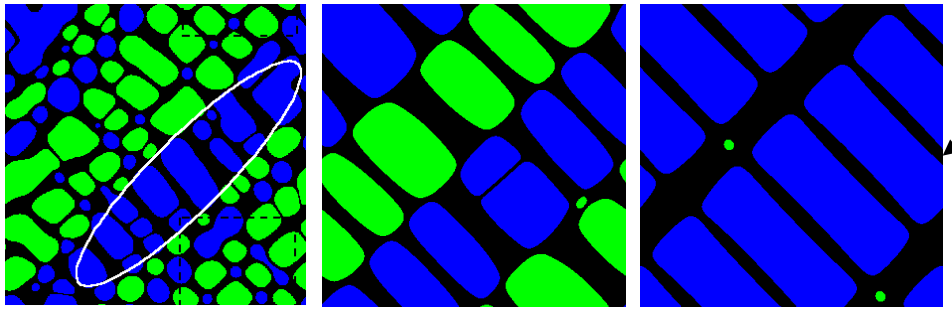

d = -0.5

d=0

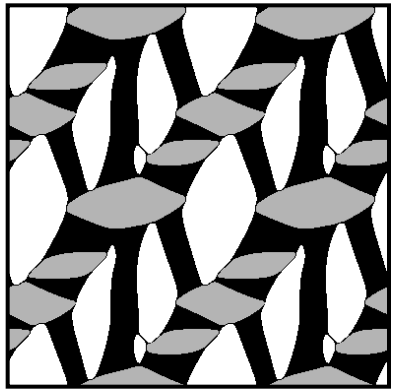

Ni-20V-10Co

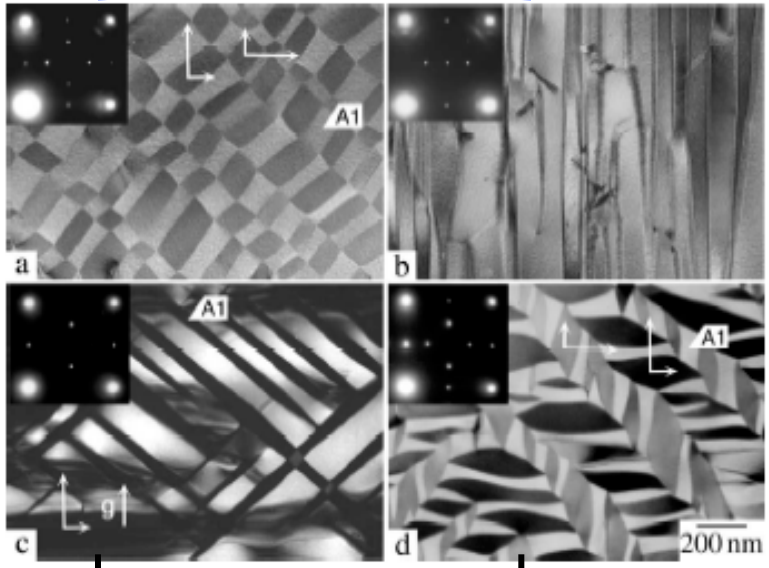

Ni-19V-4Fe

Ni-15V-5Nb

TEM images of ternaries alloys aging at 1073°K 864 ks, A1/DO_{22} microstructure
(A. Suzuki, H. Kojima, T. Matsuo and M. Takeyama, Intermetallics 12 (2004) 969-975)

H. Zapolsky,S. Ferry, X. Sauvage,D. Blavette, L.Q. Chen, Phil. Mag. (2011)
J. Boisse, H. Zapolsky, A.G. Khachaturyan Acta Mat. (2011)

Continuum version of the ADF model (Y. Jin, A.G. Khachaturyan APL(2006))

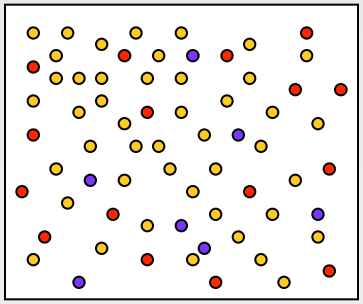

$$\frac{a}{R_{W\alpha\beta}} << 1$$

A small parameter determining the transition discrete continuum version of ADF model is:

a- Ising lattice parameter

$R_{W\alpha\beta}$- characteristic distance of interatomic interaction

ADF on constrained lattice

P(r) - probability to find atom at position r

Microscopic diffusion equation

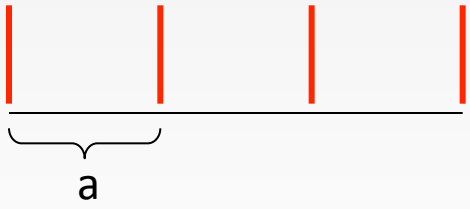

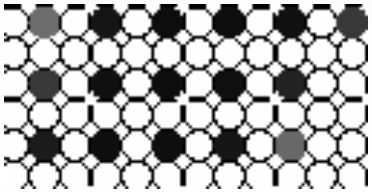

ADF on unconstrained lattice

ρ(r) - atomic density

$$\{\rho(\boldsymbol{r})_\alpha\} = (\rho_1, \rho_2, \ldots, \rho_\alpha, \ldots, \rho_n)$$

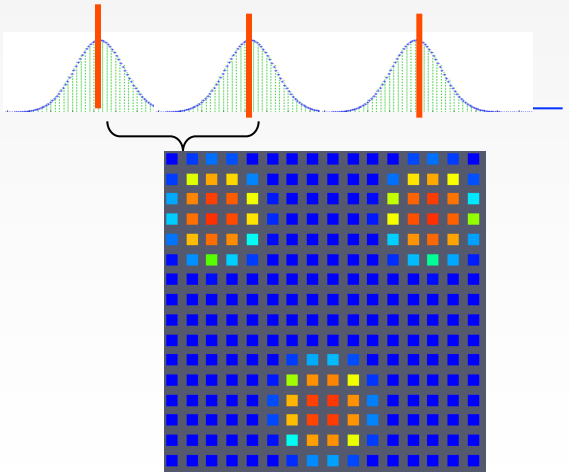

• There is no Ising lattice constraint: atoms are free to continuously move to relax the free energy.

• The n-component system is described by the *n* **atomic density functions**:

$$\{\rho(\boldsymbol{r})_\alpha\} = (\rho_1, \rho_2, \ldots, \rho_\alpha, \ldots, \rho_n)$$

• **The ADF kinetic** equations are essentially the same as a microscopic diffusion equation (A.G. Khachaturyan 1976) but the integration is over continuum space is substituted for summation over lattice sites:

$$\frac{\partial \rho_\alpha(\mathbf{r},t)}{\partial t} = \sum_{\beta=1}^{\beta=n} \int_V L_{\alpha\beta}(\mathbf{r},\mathbf{r}') \frac{\delta F}{\delta \rho_\beta(\mathbf{r}',t)} d^3 r' \qquad \alpha = 1,2,\ldots,n$$

$F(\{\rho_\alpha(\mathbf{r})\})$ is a non-local free energy functional of *n* atomic density functions, $L_{\alpha\beta}(\mathbf{r},\mathbf{r}')$ is the mobility matrix.

The conservation of the number of atoms:

$$\int_V L_{\alpha\beta}(\mathbf{r},\mathbf{r}') d^3 r' = 0.$$

Atomic density function approach

Free energy :

$$F[\{\rho_\alpha\}] = \frac{1}{2}\iint_{V\,V}\sum_{\alpha\beta} W_{\alpha\beta}(\mathbf{r}-\mathbf{r}')\rho_\alpha(\mathbf{r})\rho_\beta(\mathbf{r}')\,d^3r\,d^3r' + \int_V f(\{\rho_\alpha(\mathbf{r})\})d^3r$$

Non-local term **Local term**

The local free energy density $f(\rho_\alpha(r))$ can be approximated by the Landau polynomial expansion with respect to density $\rho_\alpha(r)$ or by entropy term.

$W_{\alpha\beta}(\mathbf{r}-\mathbf{r}')$ the effective interaction potentials

Embedded potential, effective paire potential, …

Limit transition to the Landau theory

$$F = \int \frac{1}{2} \sum_{\alpha\beta} V_{\alpha\beta}(k) \Phi_{\alpha}(k) \Phi^{*}_{\beta}(k) \frac{d^3k}{(2\pi)^3} + \int_V f(\{\rho_{\alpha}(r)\}) d^3r$$

Where $V_{\alpha\beta}(\mathbf{k})$ is the Fourier transforms of the effective potentials $W_{\alpha\beta}(\mathbf{r})$:

$$\mathrm{V}(\boldsymbol{k}) = \int_{\mathrm{V}} \mathrm{W}(\boldsymbol{r}) \exp(-\mathrm{i}\boldsymbol{k}\boldsymbol{r}) \mathrm{d}^3\mathrm{r}$$

Using Taylor expansion of $V_{\alpha\beta}(\mathbf{k})$ in k

$$V_{\alpha\beta}(k) = A_0^{\alpha\beta} + \frac{1}{2!} A_2^{\alpha\beta} k^2 + \frac{1}{4!} A_4^{\alpha\beta} k^4 + \ldots + \frac{1}{n!} A_n^{\alpha\beta}$$

Eq.(1) is a generalized **Landau gradient expression**:

$$F = \int_V \sum_{\alpha\beta} \left(\frac{1}{2!} A_o^{\alpha\beta} \rho_{\alpha}(\mathbf{r}) \rho_{\beta}(\mathbf{r}) + \frac{1}{2!} A_2^{\alpha\beta} \nabla\rho_{\alpha}(\mathbf{r}) \nabla\rho_{\beta}(\mathbf{r}) + \frac{1}{4!} A_4^{\alpha\beta} \nabla^2\rho_{\alpha}(\mathbf{r}) \nabla^2\rho_{\beta}(\mathbf{r}) + \ldots \right) d^3r + \int_V f(\{\rho(\mathbf{r})_{\alpha}\}) d^3r$$

The **Phase Field Crystal model** has used two first terms of the gradient expansion of the Landau theory.

To investigate the stability of the homogeneous state with respect to the density modulations, we can expand the free energy (1) into the Taylor series with respect to the spatial variations of the atomic densities

$$\Delta\rho_\alpha(r) = \rho_\alpha(r) - \bar{\rho}_\alpha$$

Free energy change with respect to homogeneous state is :

$$\Delta F = \frac{1}{2}\iint_V \sum_{\alpha\beta} \left[W_{\alpha\beta}(\mathbf{r}-\mathbf{r}') + \frac{\partial^2 f(\{\rho_\alpha\})}{\partial\rho_\alpha \partial\rho_\beta} \right] \Delta\rho_\alpha(\mathbf{r})\Delta\rho_\beta(\mathbf{r}')d^3r d^3r'$$

$$D_{\alpha\beta}(k,T,\{\rho_\alpha\})$$ Response function

Response function can be estimated from the elastic diffuse scattering

$$I(\mathbf{k}) \sim \left|\Phi(\mathbf{k})\right|^2$$

where Φ(k) Fourier transform of the ρ(r)

$$< \Phi_\alpha(k)\Phi^*_\beta\ (k) >= k_B T D^{-1}_{\alpha\beta}(\mathbf{k})$$

Atomic density function modeling of atomic structure of grain boundaries

$$f(\{\rho(\mathbf{r})\}) = \int \frac{d^3k}{(2\pi)^3} V(k)\rho_{\mathbf{k}}\rho_{-\mathbf{k}} + f_{\text{loc.}},$$

$$f_{\text{loc.}} = k_B T \int \frac{d^3r}{V} \left[\rho(\mathbf{r}) \ln \rho(\mathbf{r}) + (1-\rho(\mathbf{r})) \ln(1-\rho(\mathbf{r}))\right].$$

$$V(k) = V_0 \left(1 - k^4 / \left[(k^2 - {k_1}^2)^2 + {k_2}^4\right]\right)$$

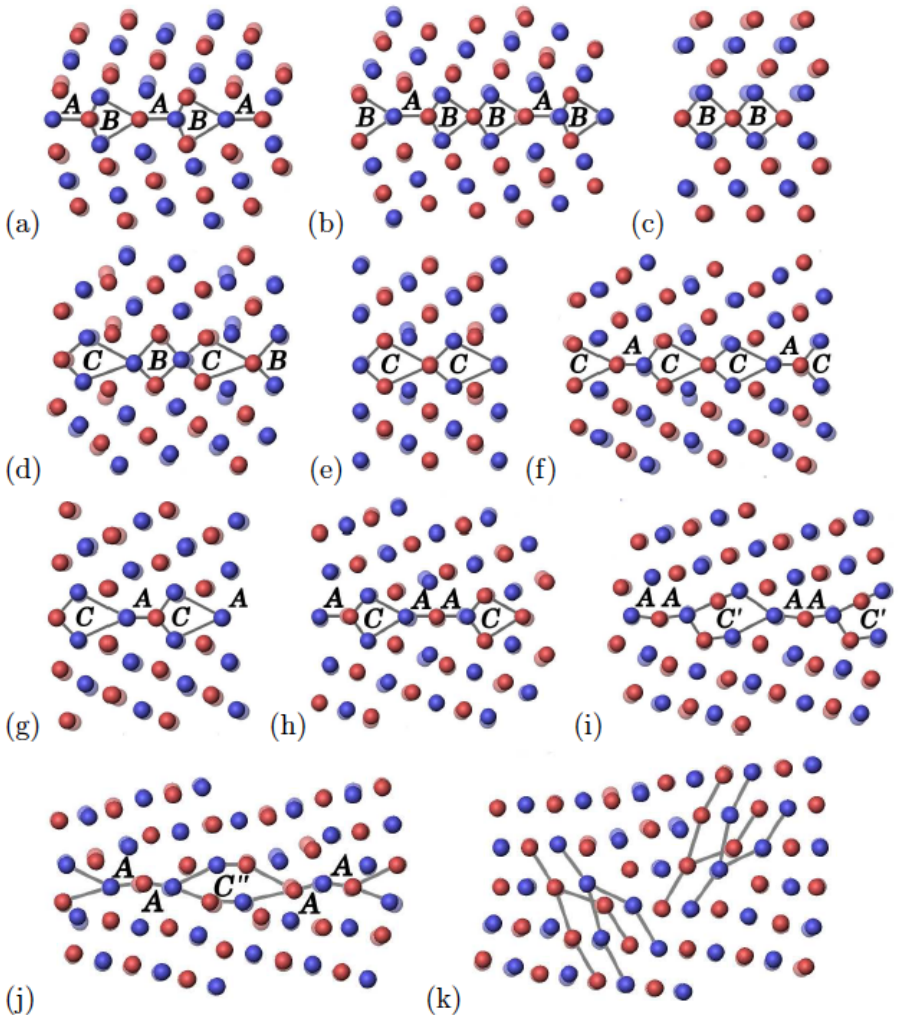

Figure 2: The structural units in ⟨110⟩ GBs modeled by the ADF: a) 38.94°, Σ9(114); b) 50.48°, Σ11(113); c) 70.53°, Σ3(112); d) 93.37°, Σ17(334); e) 109.53°, Σ3(111); f) 121.01°, Σ33(554); g) 129.52°, Σ11(332); h) 141.06°, Σ9(221); i) 148.41°, Σ27(552); j) 153.47°, Σ19(331); k) 163.9°, Σ51(551). The equilibrium atomic positions after a relaxation by MD simulation are indicated in the background with faded colors; different colors refer to two adjacent atomic planes. The last image represents dislocations.

O. Kapikranian, H. Zapolsky, C. Domain, R Patte,C.Pareige- PRB, 2014

Simulated diffraction patterns and HRTEM images of GB

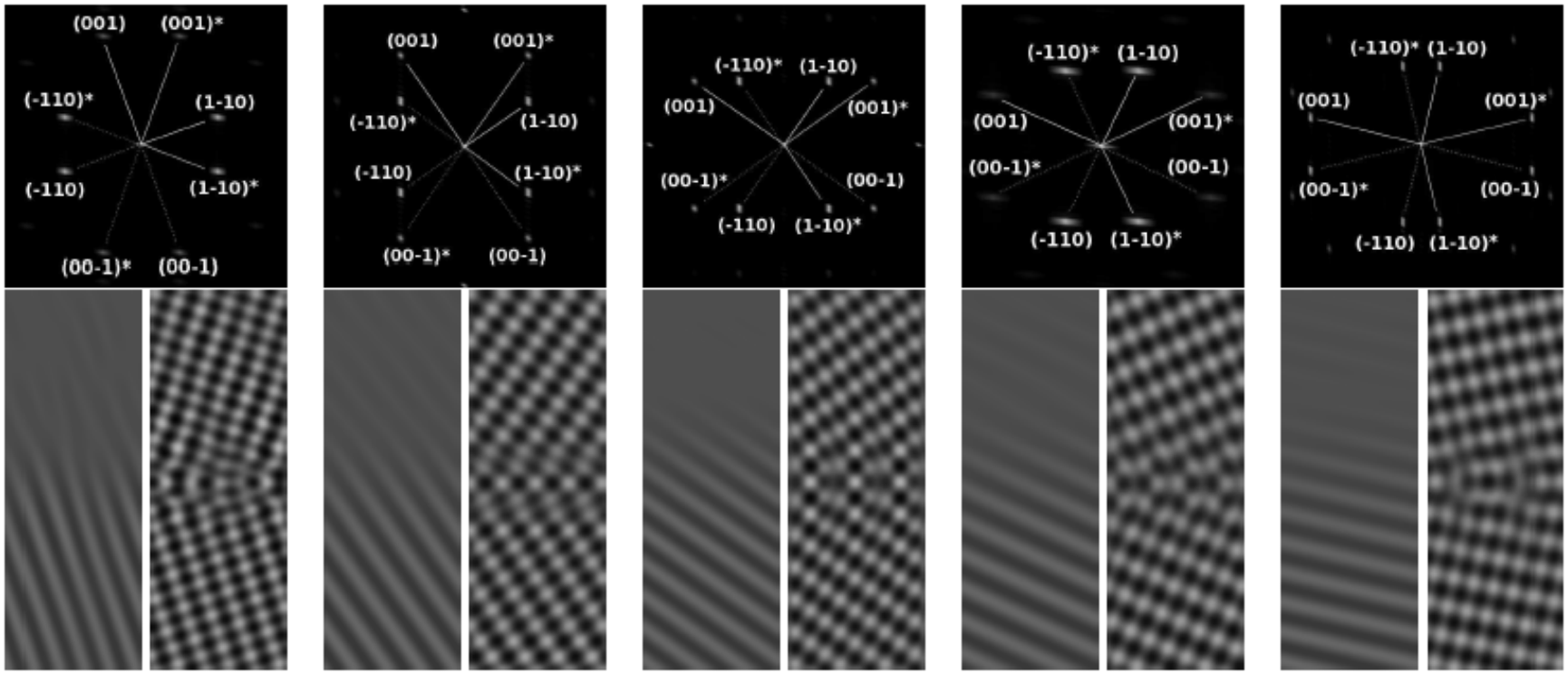

FIG. 8. Diffraction patterns (upper row), and the real space reconstruction based on the brightest spot $(1\bar{1}0)$ and its conjugate $(\bar{1}10)$ (on the left of each column) or on all the spots indicated in the diffraction patterns (on the right of each column) for a [110] tilt GB of (a) 38° (Σ9(114)); (b) 70° (Σ3(112)); (c) 109.53° (Σ3(111)); (d) 129° (Σ11(332)); (e) 153°, (Σ19(221)).

FCC structure

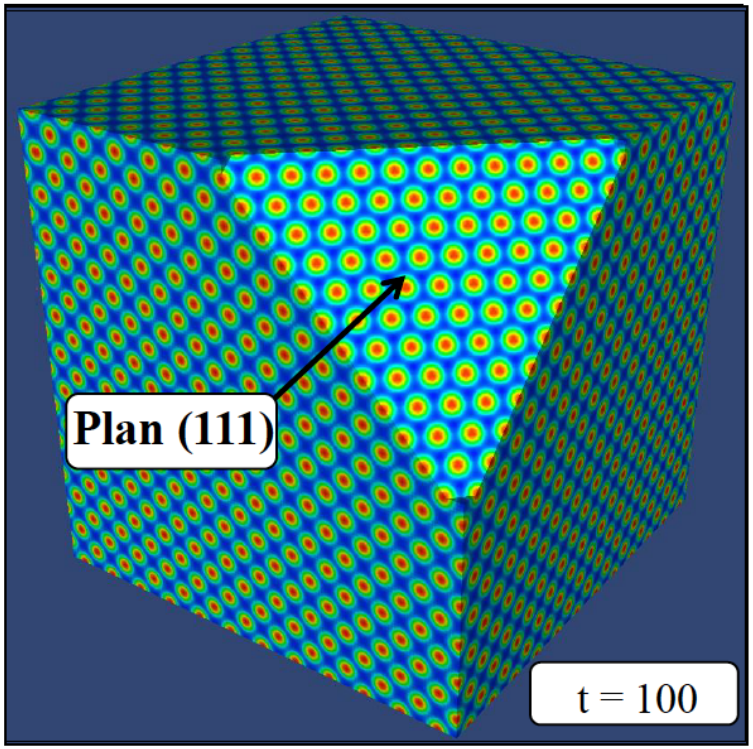

$$V_{CFC}(k) = \min \begin{cases} V_0 \left[1 - \dfrac{(k/\epsilon_1)^4}{((k/\epsilon_1)^2 - \kappa_1^2) + \kappa_2^4} \right] \\ V_0 \left[1 - \dfrac{(k/\epsilon_2)^4}{((k/\epsilon_2)^2 - \kappa_1^2) + \kappa_2^4} \right] \end{cases}$$

$$\epsilon_1 = 1 \quad \epsilon_2 = 2/\sqrt{3}$$

$$\kappa_1 = 0.97 \quad k_2 = 0.485 \quad V_0 = 1/17$$

FCC to BCC transition
ADF modeling

Initial configuration –> bcc nucleus (r=20Δ) with KS orientation relation with the fcc parent phase

$$\frac{a_0^{FCC}}{a_0^{BCC}} = \sqrt{\frac{3}{2}} \approx 1.225$$

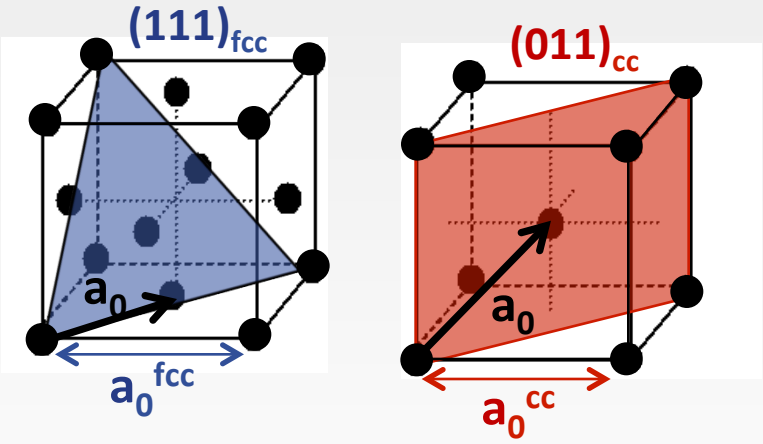

Fe_α : a_0 = 2,886
Fe_γ: a_0 = 3,6
} ≈1.247

Fe-Ni-C : - BCC : a_0 = 2,845
- FCC : a_0 = 3,592
} ≈1,263

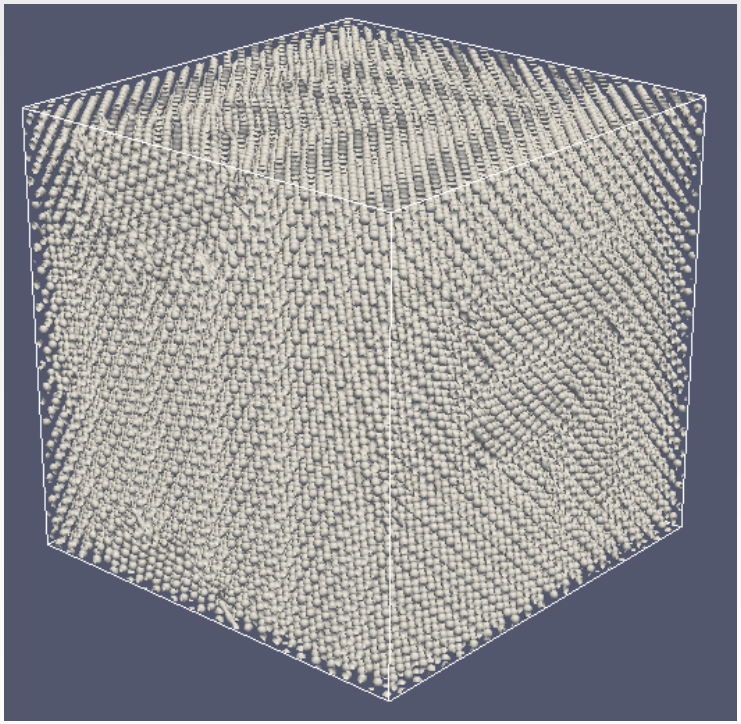

t*=9000
Simulation box: 256^3

FCC to BCC transition. ADF modeling

Case II

Bcc embryo r=20Δ

fcc/bcc K-S relation

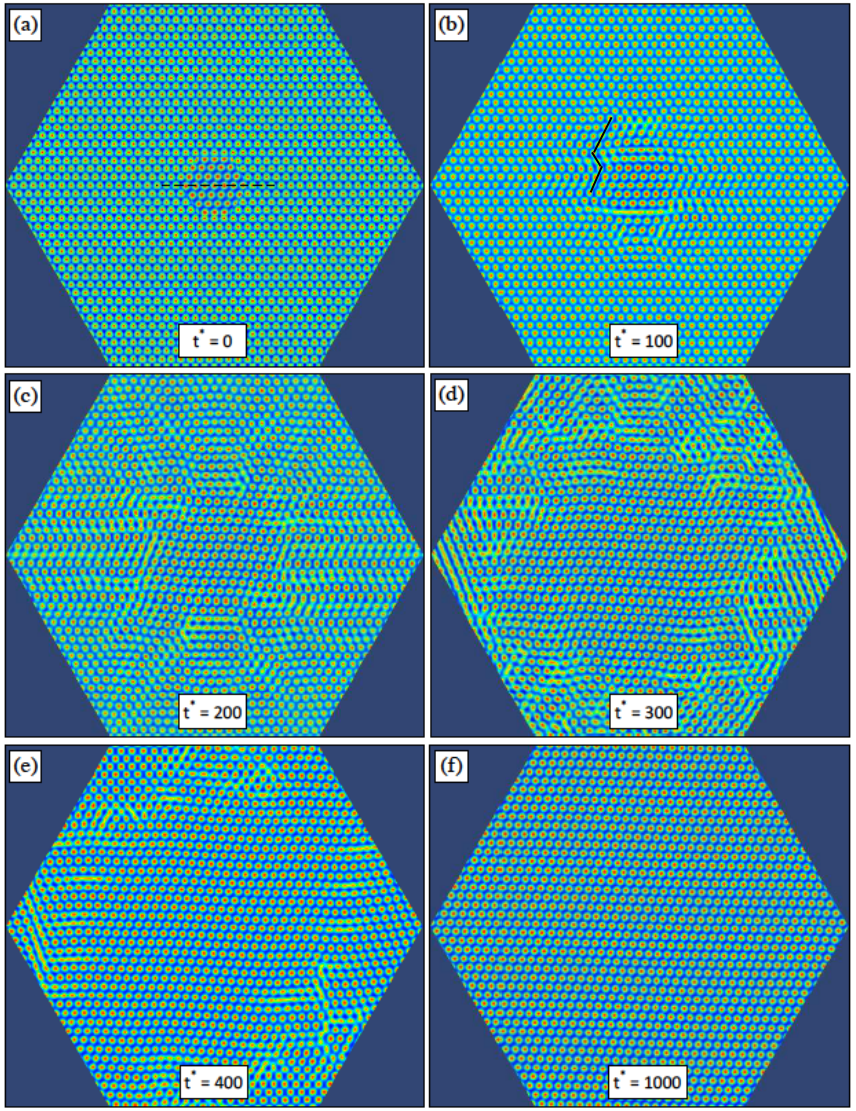

FCC to BCC transition.
ADF modeling

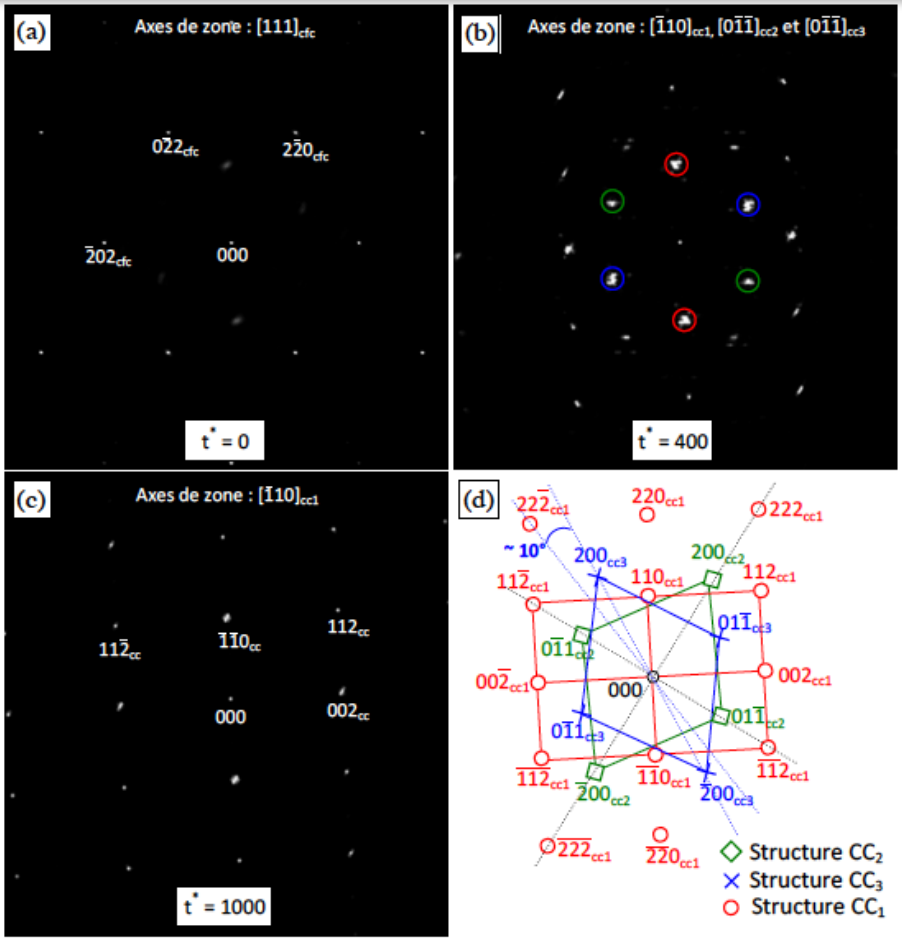

$$\left((\bar{1}\,10)_{cc1}, (0\,\bar{1}\,\bar{1})_{cc2}\right) \approx 10° \quad \text{et} \quad [\bar{1}\,10]_{cc1} \,//\, [0\,\bar{1}\,\bar{1}]_{cc3}$$

Simulated diffraction pattern

FCC to BCC transition. ADF modeling
Dark-field images

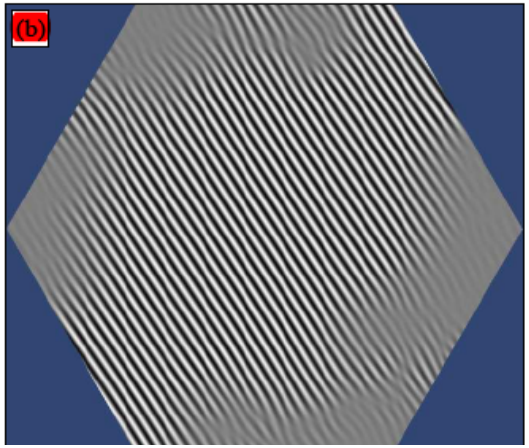

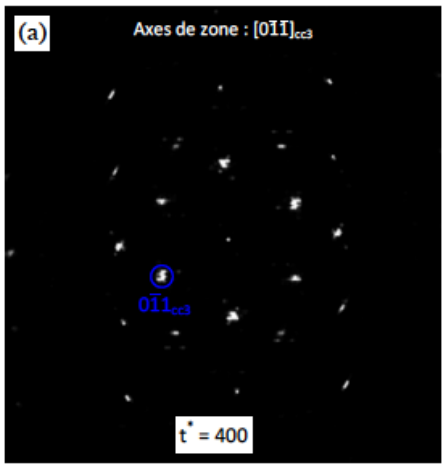

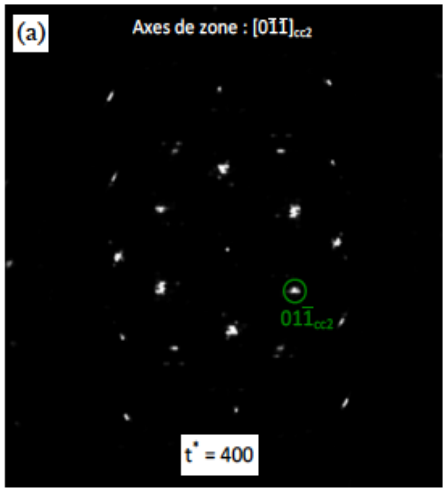

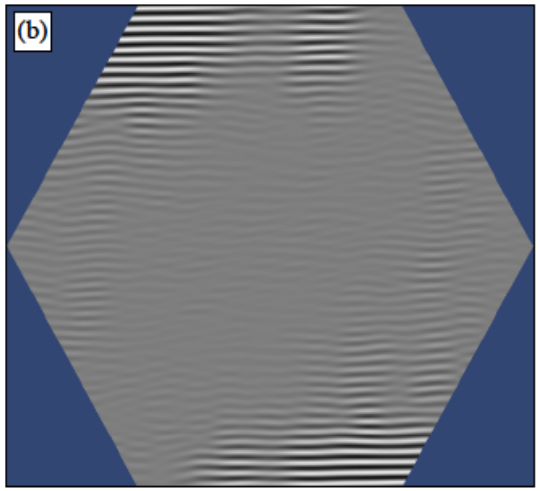

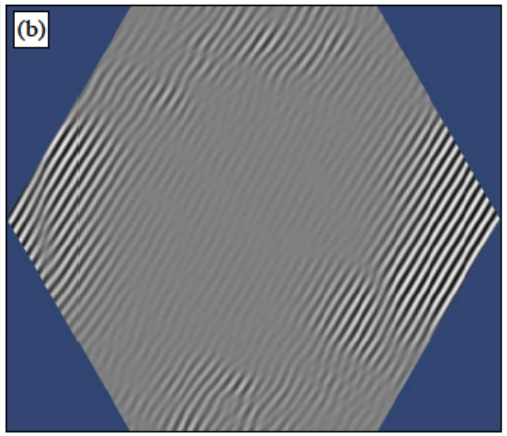

FCC to BCC transition. ADF modeling
Slip planes

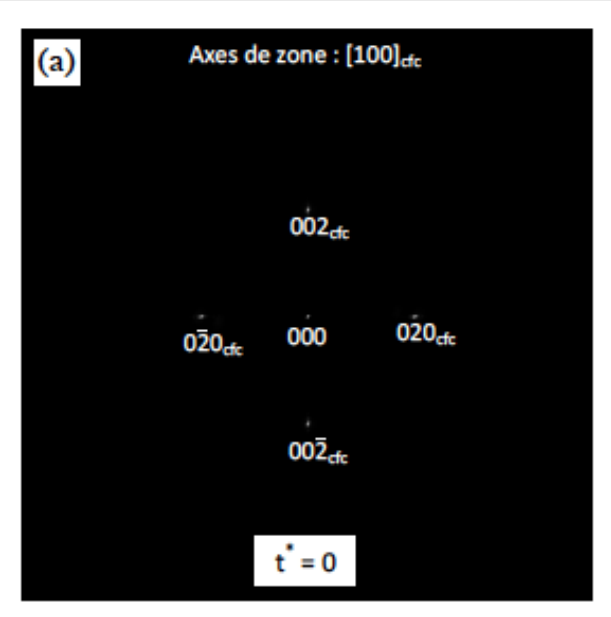

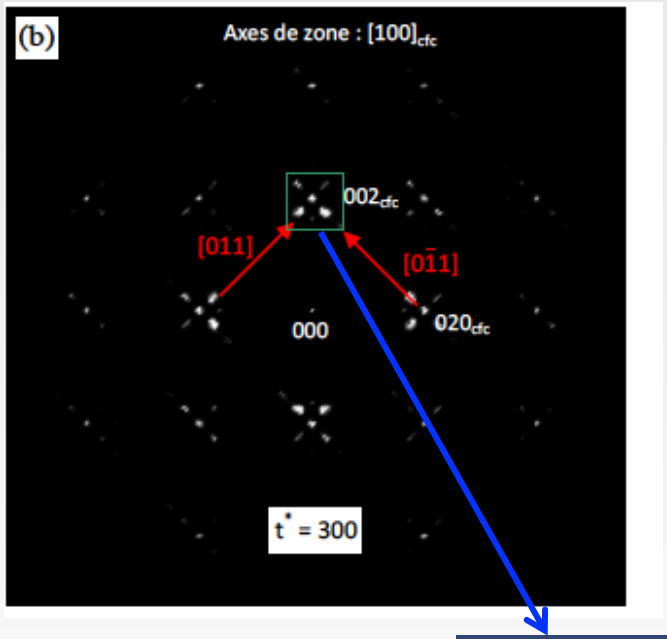

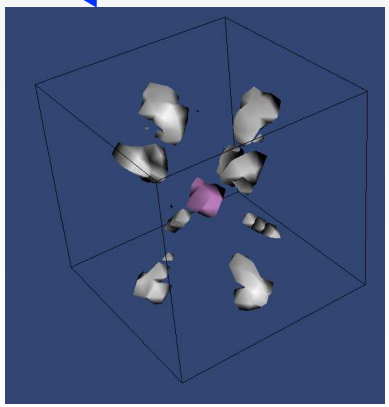

FCC to BCC transition. ADF modeling. 110 slip planes

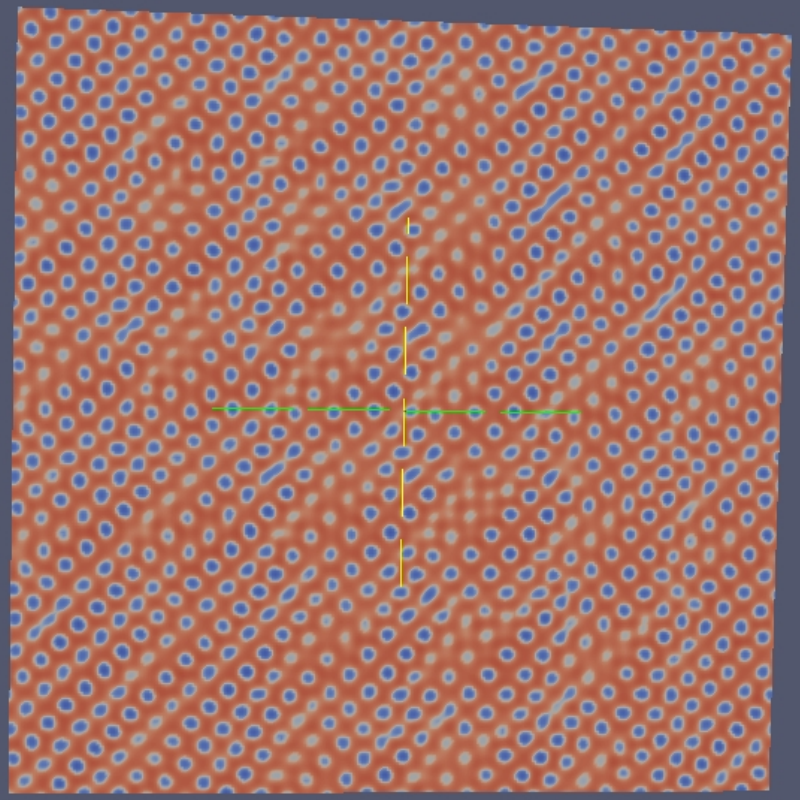

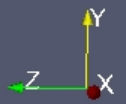

FCC to BCC transition. ADF modeling
FCC stable phase

$$V_1(k) = V_0\left[1-\left(\frac{(k/\varepsilon_1)^4}{((k/\varepsilon_1)^2-\kappa_1^2)^2+\kappa_2^4}\right)\right]$$

$$V_2(k) = V_1\left[1-\left(\frac{(k/\varepsilon_2)^4}{((k/\varepsilon_2)^2-\kappa_1^2)^2+\kappa_2^4}\right)\right]$$

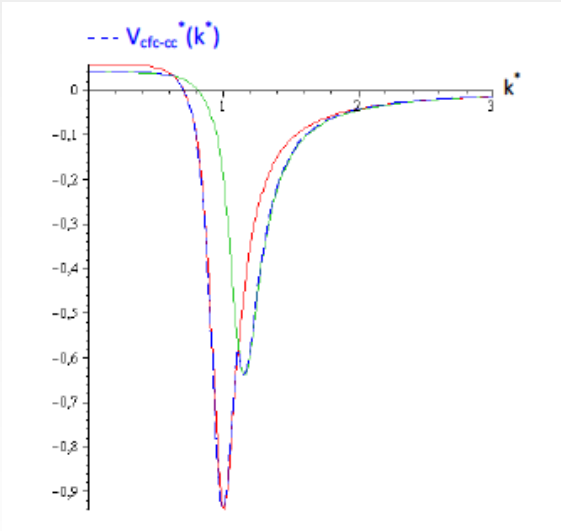

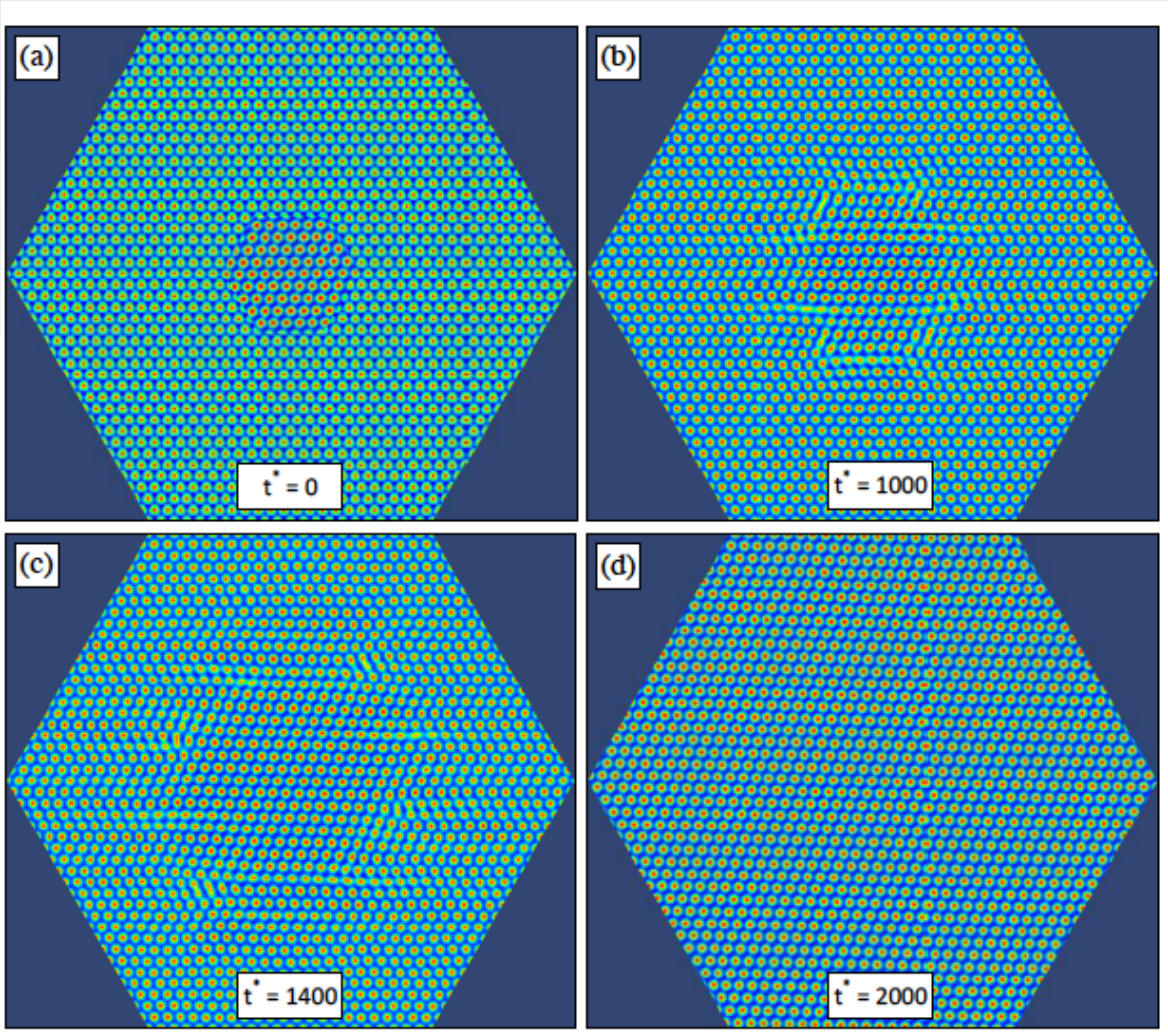

FCC to BCC transition. ADF modeling

Diffraction at $t = 400$

Zone axes: $[111]_{fcc}$

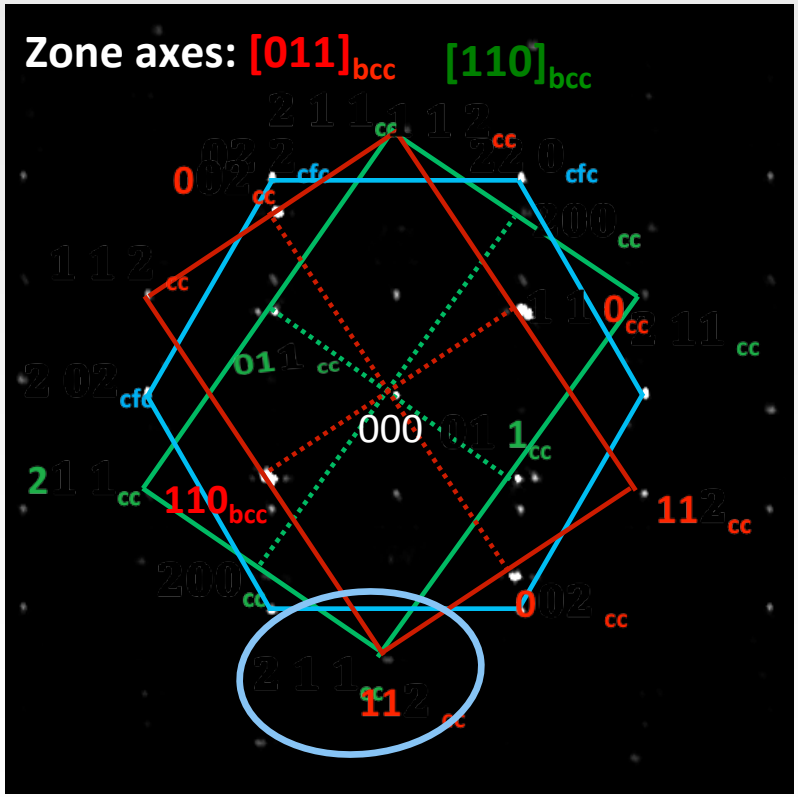

→ FCC structure

→ BCC (nucleus)

→ second variant of the BCC structure

➡ Two variants with twin relation $\{112\}$

Fe-Ni alloy

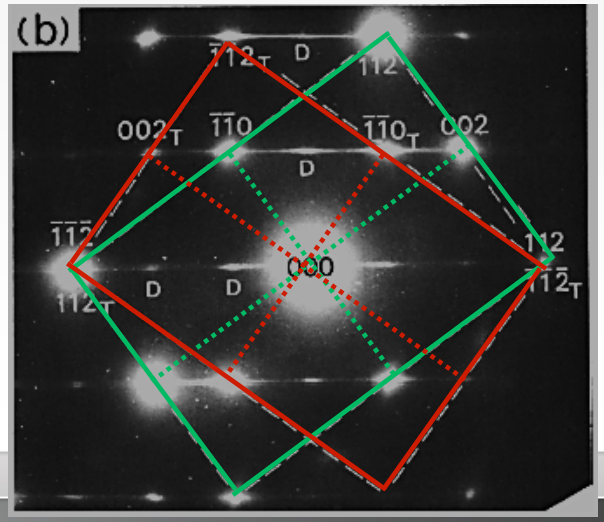

➡ Good agreement with experimental data

K. Shimizu & Z. Niskyama Chen & Met. Mat. Trans. B (1972)

Localisation of two BCC variants

➡ **Evolution of dark field images:**

(111) plane

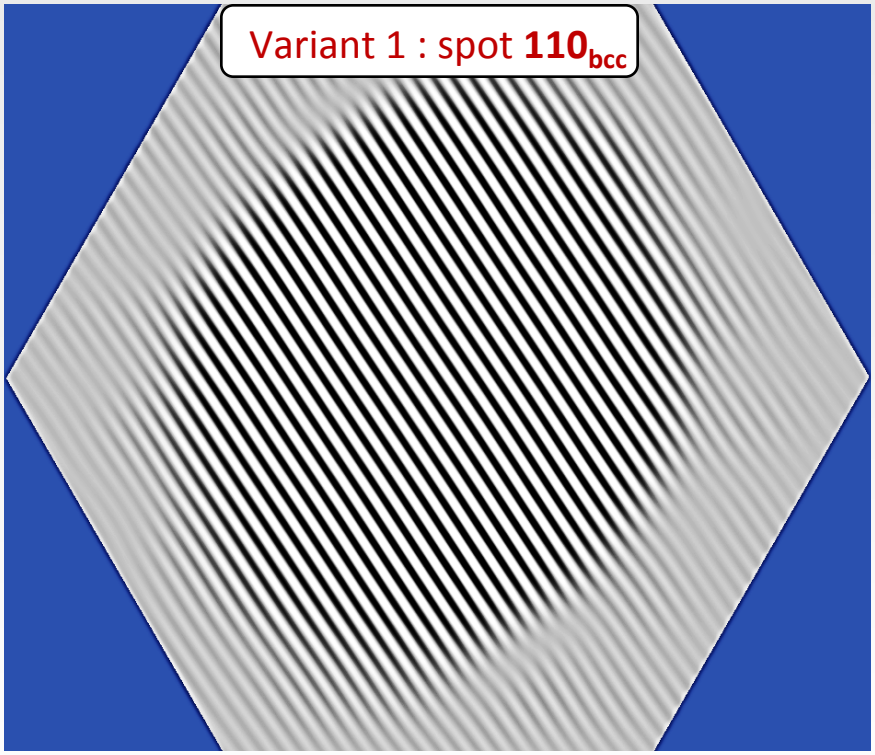

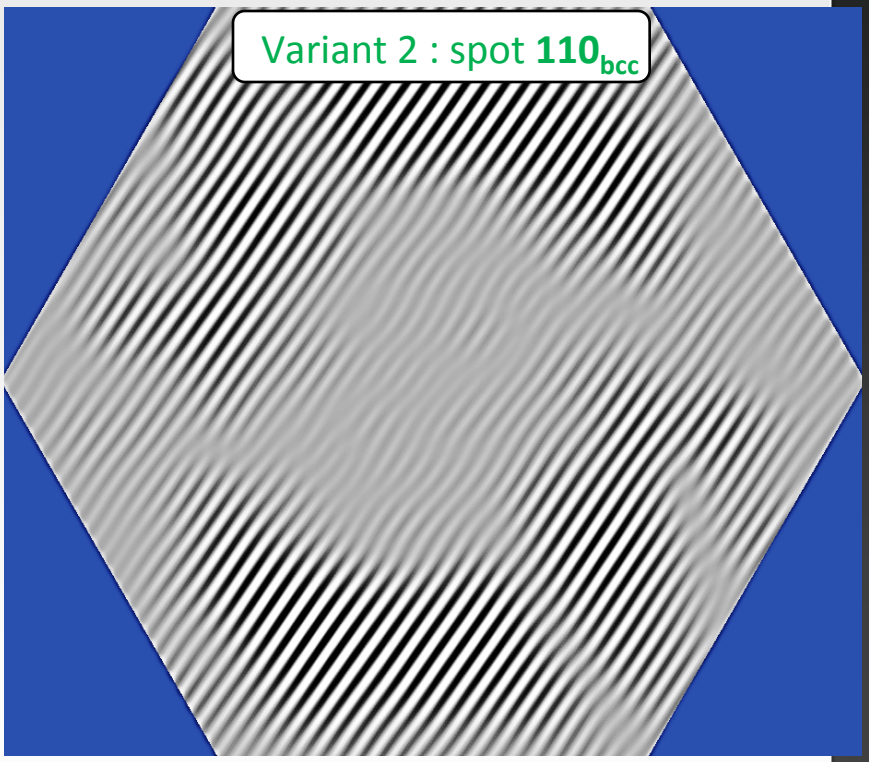

t = 1600

➡ **Second BCC variant is situated at the interface between the first variant and the matrice**

Shape of two variants martensite nucleus

3D dark field image

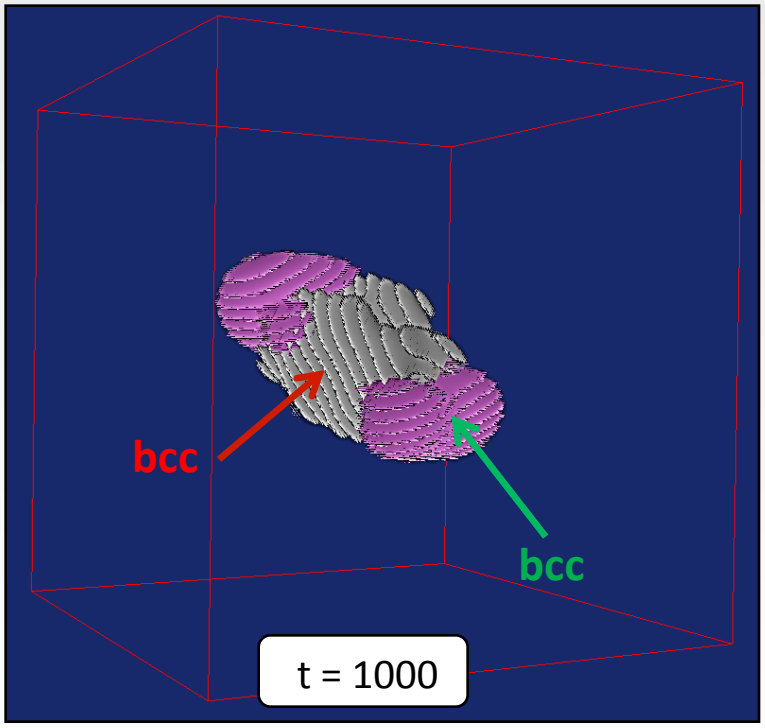

plan (100)

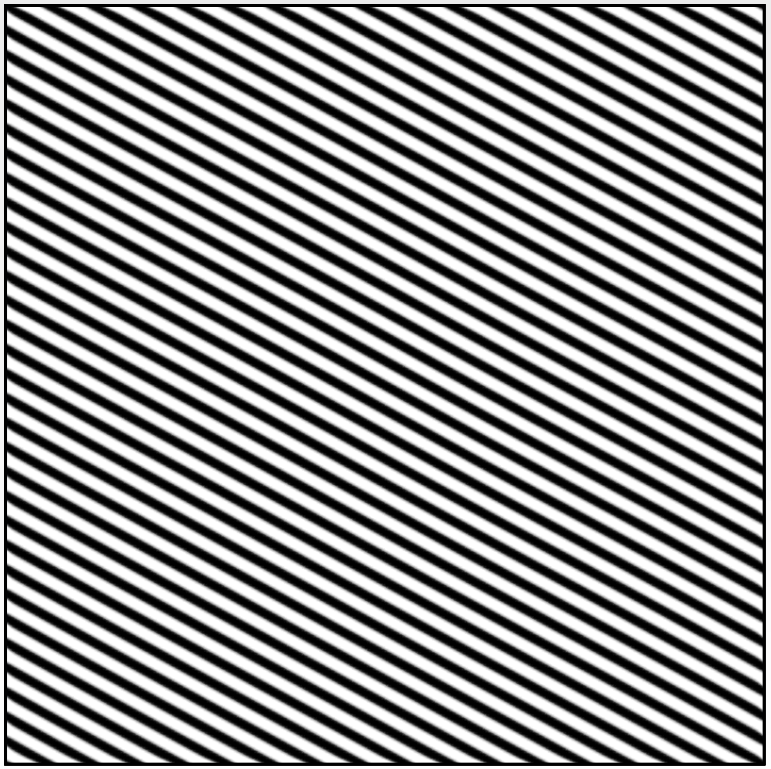

The nucleus growth in a plate form

CONCLUSIONS

- ***The ADF model previously developed to describe the decomposition and ordering on the Ising lattice is applied to the general case of the microstructural evolution with arbitrary atomic movements.***

- ***The main results of this modeling is the finding that the pre-existing martensitic nucleus never had a single-domain structure. The martensite nucleus is the multivariant structure which depends from the stability of the fcc phase.***

THANK YOU FOR ATTENTION

GPM
Groupe de Physique des Matériaux